TÜBİTAK

Turkish Journal of Electrical Engineering & Computer Sciences

http://journals.tubitak.gov.tr/elektrik/

Research Article

Turk J Elec Eng & Comp Sci
(2017) 25: 3052 – 3060

doi:10.3906/elk-1608-285

Energy and area spectral efficiency trade-off for MC-CDMA with carrier frequency offset

Junaid AHMED[1,*], **Moazzam Islam TIWANA**[1], **Omar AHMAD**[1], **Sarmad SOHAIB**[2]
[1]Department of Electrical Engineering, COMSATS Institute of Information
Technology, Tarlai Kalan, Islamabad, Pakistan
[2]Department of Electrical Engineering, University of Engineering and
Technology, Taxila, Pakistan

Received: 26.08.2016 • **Accepted/Published Online:** 02.12.2016 • **Final Version:** 30.07.2017

Abstract: Intercell interference is a major factor that limits the capacity of cellular wireless communication systems. This paper proposes an accurate statistical model that caters to interference and noise to determine the ergodic capacity. A new expression for ergodic capacity is derived that enables us to calculate area spectral efficiency (ASE) and energy efficiency (EE). This expression has been used to calculate and compare ASE and EE for low and high traffic scenarios with various signal-to-noise ratios and intercell distances.

Key words: Intercell interference, energy efficiency, area spectral efficiency, MC-CDMA, carrier frequency offset

1. Introduction

Multicarrier code-division multiple-access (MC-CDMA) is a promising access technology for the development of future wireless networks. It combines the advantages of both orthogonal frequency division multiplexing (OFDM) and wideband CDMA (WCDMA). Not only does it offer high data rates and high spectral efficiency, but it is also resistant to frequency selective fading and narrow band jamming signals. In this technology, the signal is first spread in the frequency domain and then transmitted over multiple carriers using modulation. However, one of the major disadvantages of this technique is that it suffers from multiple-access interference (MAI), which results in performance degradation. The issues related to MAI have been extensively studied in the literature [1–12].

Communication systems around the world consume huge amounts of electricity. For example, in Italy around 1% of total electricity produced is consumed by telecommunication networks [13]. Hence, the total amount of electricity consumed by them amounts to 2 TWh per year and it is expected to increase 10-fold over the next 10 years. Similarly, there has been an enormous growth in mobile network infrastructure [14] around the world. This increase in demand as well as the cost of electricity has resulted in engineers trying to design networks that are more energy-efficient. A combination of hardware and software techniques are being researched and used to achieve this. As an example, the 2G GSM Base Station (BS) requires power of 800 W for its operation while the 3G BS requires 430 W [15]. This is important as the BS uses about 80% of the electricity consumed by a mobile network [13, 14]. One of the techniques to further reduce electricity consumption is to put BSs/cells with low traffic into sleep mode [16], while their subscribers may be provided

---

[*] Correspondence: junaid@comsats.edu.pk

coverage by the neighboring active cells. However, this approach has a disadvantage as the neighboring active cells have to increase their transmit power. As a result, the user equipment (UE) also transmits with more power and drains out quickly. Similarly, the UE may also experience a decrease in quality of service (QoS) as it switches from current to neighboring cells. It is important to decrease the carbon emission of wireless networks; it already represents 0.2% of carbon dioxide emissions and this is expected to double by 2020 [17]. Aldosari et al. [18] proposed a novel method of calculating the ergodic capacity of cellular systems and also investigated the trade-off between area spectral efficiency (ASE) and energy efficiency (EE). In this paper, a similar approach has been adopted to derive a new accurate expression for the ergodic capacity of downlink cellular MC-CDMA systems in the presence of carrier frequency offset, which, to our knowledge, has not been done before. The new expression is then used to compare and analyze ASE and EE for both high and low traffic scenarios. This paper has the following important contributions:

- A novel expression has been derived for the calculation of ergodic capacity for a basic 7-cell downlink cellular MC-CDMA cellular model.
- Calculations and comparisons have been made for this cellular model using ASE and EE.
- All the results have been verified using Monte Carlo simulation.

2. System model

Consider a 7-cell cellular system as shown in Figure 1, with a frequency reuse factor of 1, where each BS communicates using MC-CDMA in the downlink. Due to the unit frequency reuse factor, each user will experience interference from all cells in the neighborhood; however, for simplicity we shall only consider the immediate 6 neighbors. This assumption is justified as the interference from the subsequent neighbors will only be a fraction of the interference from the immediate neighbors due to their distance. All users are considered to be uniformly distributed in the cell with the BS at the center. The downlink composite signal transmitted by the BS consists of orthogonally combined signals for all users in the cell, whereas the signal for each user in a typical signaling interval T is given by

$$s(t) = \frac{1}{\sqrt{N_p}} \sum_{n=0}^{N_p-1} b\left(t\right) c\left[n\right] \mathrm{e}^{j2\pi f_n t}, \;\; t \in \left[-T_g, T\right], \tag{1}$$

where N_p is the processing gain, which also equals the number of subcarriers; $b(t)$ is the information-bearing signal; $c[n]$ is the spreading code and we assume that an orthogonal spreading code is used; f_n is the center frequency of the nth subcarrier; and T_g is the length of the cyclic prefix. The received signal $R_c(t)$ at a typical user at a distance r from the BS is given by

$$\begin{aligned} R_c(t) \;\; = \;\; & \frac{1}{\sqrt{N_p}} r^{-\beta} \sum_{n=0}^{N_p-1} G_n\, b\left(t\right) c\left[n\right] \mathrm{e}^{j2\pi f_n t} + \sum_{k=1}^{6} \frac{1}{\sqrt{N_p}} r_k^{-\beta} \\ & \times \sum_{n=0}^{N_p-1} G_{n,k}\, b_k\left(t\right) c_k\left[n\right] \mathrm{e}^{j2\pi f_n t} \mathrm{e}^{j2\pi \frac{\triangle_k}{T} t} + \eta\left(t\right), \end{aligned} \tag{2}$$

where the first term is the desired signal from its own BS. The second term is interference from the six neighboring base stations, where the subscript k represents one of the six neighbors. We consider the worst-case scenario

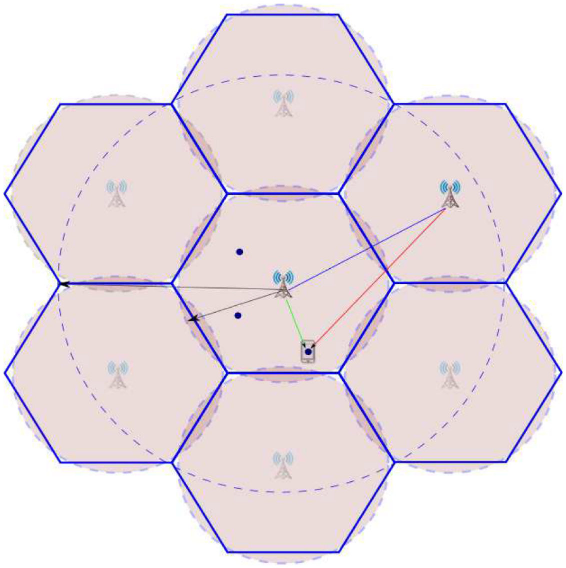

Figure 1. Cellular model.

where all six neighboring BSs are utilizing the same subcarriers in the given time interval. No interference is assumed from the signals for other users in the same BS, as the user is assumed to be phase-locked with its base station; however, there is a frequency offset of Δ_k with the neighboring base stations, which results in interference. The last term $\eta(t)$ in Eq. (2) represents AWGN, β represents the path loss factor, and G_n and $G_{n,k}$ are channel transfer functions. We assume a frequency-selective, multipath Rayleigh fading channel; therefore, all G_n and $G_{n,k}$ are zero mean complex Gaussian random variables with unit variance. In Eq. (2) r_k is the distance between the user and the kth neighboring BS; it can be written in terms of the distance between two BSs R as follows:

$$r_k = \sqrt{R^2 + r^2 - 2Rr\cos(\theta)}, \tag{3}$$

where θ is shown in Figure 1. The received signal is decoded by a conventional correlation receiver with maximal ratio combining. Let Z represent the receiver decision variable; then

$$Z = \sum_{m=0}^{N_p-1} \frac{1}{T} \int_0^T G_m^* \, c\,[m]\, \mathrm{e}^{-j2\pi f_m t}\, r\,(t)\, dt. \tag{4}$$

Z can be separated into three distinct components, $Z = S + I + N$, where S is the desired signal component, I is the intercell interference component, and N is the AWGN component. These are given as follows:

$$S = \sqrt{\frac{r^{-\beta}}{N_p}} b(t) \sum_{m=0}^{N_p-1} |G_m|^2, \tag{5}$$

$$I=\sum_{m=0}^{N_p-1}\frac{1}{T}\int\limits_{0}^{T}G_m^{*}c\left[m\right]\mathrm{e}^{-j2\pi f_m t}\sum_{k=1}^{6}\sqrt{\frac{r_k^{-\beta}}{N_p}}\sum_{n=0}^{N_p-1}G_{n,k}b_k(t)c_k\left[n\right]\mathrm{e}^{j2\pi f_n t}\mathrm{e}^{j2\pi\frac{\triangle_k}{T}t}dt. \tag{6}$$

If no frequency offset between BSs is assumed, then $\Delta_k=0$ and it can be shown that the interference component I becomes zero. Therefore, if frequency offset is ignored there is no interference in the downlink, but this is not a practical assumption. The integration in (6) can be solved to get

$$I=\sum_{m=0}^{N_p-1}G_m^{*}c\left[m\right]\sum_{k=1}^{6}\sqrt{\frac{r_k^{-\beta}}{N_p}}\sum_{n=0}^{N_p-1}G_{n,k}b_k(t)c_k\left[n\right]\frac{\mathrm{e}^{j2\pi(n-m+\triangle_k)}-1}{j2\pi(n-m+\triangle_k)}. \tag{7}$$

Note that I in Eq. (7) is a large sum of independent zero mean random variables and therefore Z can be considered as a Gaussian random variable. The mean of Z has a contribution from S only as I and N are zero mean random variables, and it can be written as follows:

$$\mathbb{E}\left[Z\right]=\sqrt{\frac{r^{-\beta}E_s}{N_p}}\left(\sum_{m=0}^{N_p-1}\left|G_m\right|^2\right), \tag{8}$$

where $\mathbb{E}\left[\right]$ is the expectation operator and E_s is the signal energy. The variance ($\mathbb{V}\left[\right]$) can be found as

$$\mathbb{V}\left[Z\right]=\sum_{k=1}^{6}\frac{r_k^{-\beta}}{N_p}E_s\sum_{m=0}^{N_p-1}\sum_{n=0}^{N_p-1}\left|G_m^{*}\right|^2\left|G_{n,k}\right|^2\xi_{m,n}^2+\sum_{m=0}^{N_p-1}\left|G_m\right|^2N_0, \tag{9}$$

where $\xi_{m,n}^2=\mathbb{E}\left[\left|\frac{\mathrm{e}^{j2\pi(n-m+\triangle_k)}-1}{j2\pi(n-m+\triangle_k)}\right|^2\right]=\mathbb{E}\left[\mathrm{sinc}^2\left(\pi(n-m+\triangle_k)\right)\right]$, and the expectation is over Δ_k. The instantaneous signal-to-interference and noise ratio (SINR) is therefore given by the ratio

$$SINR=\frac{\frac{r^{-\beta}}{N_p}\left(\sum\limits_{m=0}^{N_p-1}\left|G_m\right|^2\right)^2}{\sum_{k=1}^{6}\frac{r_k^{-\beta}}{N_p}\sum_{m=0}^{N_p-1}\sum_{n=0}^{N_p-1}\left|G_m^{*}\right|^2\left|G_{n,k}\right|^2\xi_{m,n}^2+\sum_{m=0}^{N_p-1}\left|G_m\right|^2\frac{N_0}{E_s}}. \tag{10}$$

The instantaneous SINR expression is not affected by the spreading code used, as long as an orthogonal code is used.

The ergodic (average) capacity can be found using the Shannon capacity formula $C=\mathbb{E}\left[\log_2\left(1+SINR\right)\right]$ [bits/s/Hz]. The direct method to solve for C would require $6\times N_p\times N_p$ numerical integrations, which would make it very complicated. In the next section we employ a conditional expression and a useful lemma to solve for the ergodic capacity.

3. Ergodic capacity

The ergodic capacity expression can be written in terms of conditional capacity $C(r,\theta)$ as

$$C = \log_2(\mathrm{e}) \int_0^{R/2} \int_0^{2\pi} C(r,\theta)\, \frac{4r}{\pi R^2} d\theta dr, \tag{11}$$

since the pdf of r is $f_r(r) = 8r/R^2$ for $0 < r < R/2$, because the user is equally likely to be anywhere around the BS. Similarly, $f_\theta(\theta) = 1/2\pi$, for $0 \le \theta \le 2\pi$. Note that in Eq. (11) $C(r,\theta) = \mathbb{E}\left[\ln(1 + SINR)\,|r\right]$.

Using Lemma 1 in [18], $C(r,\theta)$ can be written as

$$\begin{aligned} C(r,\theta) \quad = \quad & \int_0^\infty \tfrac{1}{z} \exp\left(-zN_p \tfrac{N_0}{E_s}\right) \left(1 - \mathbb{E}\left[\exp\left(-zr^{-\beta} \sum_{m=0}^{N_p-1} |G_m|^2\right) |r\right]\right) \\ & \times \prod_{k=1}^{6} \mathbb{E}\left[\exp\left(-zr_k^{-\beta} \sum_{m=0}^{N_p-1} \sum_{n=0}^{N_p-1} \frac{|G_m^*|^2 |G_{n,k}|^2 \xi_{m,n}^2}{\sum_{m=0}^{N_p-1} |G_m|^2}\right) |r\right]. \end{aligned} \tag{12}$$

Assuming all channel gains are independent and applying Jensen's inequality, Eq. (12) can be simplified as

$$\begin{aligned} C(r,\theta) \quad \ge \quad & \int_0^\infty \tfrac{1}{z} \exp\left(-zN_p \tfrac{N_0}{E_s}\right) \left(1 - \prod_{m=0}^{N_p-1} \mathbb{E}\left[\exp\left(-zr^{-\beta}|G_m|^2\right) |r\right]\right) \\ & \times \prod_{k=1}^{6} \prod_{m=0}^{N_p-1} \prod_{n=0}^{N_p-1} \mathbb{E}\left[\exp\left(-zr_k^{-\beta} \frac{|G_m^*|^2 |G_{n,k}|^2 \xi_{m,n}^2}{\mathbb{E}\left[\sum_{m=0}^{N_p-1} |G_m|^2\right]}\right) |r\right]. \end{aligned} \tag{13}$$

In Eq. (13), $\sum_{m=0}^{N_p-1} |G_m|^2$ is chi-square distributed with N_P degrees of freedom. Therefore, $\mathbb{E}\left[\sum_{m=0}^{N_p-1} |G_m|^2\right] = N_p$, and Eq. (13) can be further simplified as

$$\begin{aligned} C(r,\theta) \quad \ge \quad & \int_0^\infty \tfrac{1}{z} \exp\left(-zN_p \tfrac{N_0}{E_s}\right) \left(1 - \prod_{m=0}^{N_p-1} \mathbb{E}\left[\exp\left(-zr^{-\beta}|G_m|^2\right) |r\right]\right) \\ & \times \prod_{k=1}^{6} \prod_{m=0}^{N_p-1} \prod_{n=0}^{N_p-1} \mathbb{E}\left[\exp\left(-\tfrac{zr_k^{-\beta}}{N_p} |G_m^*|^2 |G_{n,k}|^2 \xi_{m,n}^2\right) |r\right]. \end{aligned} \tag{14}$$

For a Rayleigh distributed random variable $|G_m|$ with $\sigma = 1/\sqrt{2}$,

$$\mathbb{E}\left[\exp\left(-zr^{-\beta}|G_m|^2\right) |r\right] = \frac{1}{1 + zr^{-\beta}}, \tag{15}$$

and

$$\mathbb{E}\left[\exp\left(-\frac{zr_k^{-\beta}}{N_p} |G_m^*|^2 |G_{n,k}|^2 \xi_{m,n}^2\right) |r\right] = \frac{\exp\left(\frac{N_p}{2zr_k^{-\beta}\xi_{m,n}^2}\right) N_p}{2zr_k^{-\beta}\xi_{m,n}^2} \mathrm{E}_1\left[\frac{N_p}{2zr_k^{-\beta}\xi_{m,n}^2}\right], \tag{16}$$

where E_1 is an exponential integral function given as $\mathrm{E}_1[x] = \int_x^\infty \frac{e^{-t}}{t} dt$, substituting Eqs. (15) and (16) in Eq. (14) we get

$$\begin{aligned} C\left(r,\theta\right) \quad \geq \quad & \int_0^\infty \tfrac{1}{z} \exp\left(-zN_p \tfrac{N_0}{E_s}\right) \left(1 - \left(\tfrac{1}{1+zr^{-\beta}}\right)^{N_p}\right) \\ & \times \prod_{k=1}^{6} \prod_{m=0}^{N_p-1} \prod_{n=0}^{N_p-1} \frac{\exp\left(\frac{N_p}{2zr_k^{-\beta}\xi_{m,n}^2}\right) N_p}{2zr_k^{-\beta}\xi_{m,n}^2} \mathrm{E}_1 \left[\frac{N_p}{2zr_k^{-\beta}\xi_{m,n}^2}\right] dz. \end{aligned} \tag{17}$$

Since all surrounding BSs are statistically similar and therefore will have the same net effect, Eq. (17) can be simplified as

$$\begin{aligned} C\left(r,\theta\right) \quad \geq \quad & \int_0^\infty \tfrac{1}{z} \exp\left(-zN_p \tfrac{N_0}{E_s}\right) \left(1 - \left(\tfrac{1}{1+zr^{-\beta}}\right)^{N_p}\right) \\ & \times \left(\prod_{m=0}^{N_p-1} \prod_{n=0}^{N_p-1} \frac{\exp\left(\frac{N_p}{2zr_k^{-\beta}\xi_{m,n}^2}\right) N_p}{2zr_k^{-\beta}\xi_{m,n}^2} \mathrm{E}_1 \left[-\frac{N_p}{2zr_k^{-\beta}\xi_{m,n}^2}\right] \right)^6 dz. \end{aligned} \tag{18}$$

Replacing the expression for $C\left(r,\theta\right)$ in Eq. (18) into Eq. (11) gives a much reduced expression for the ergodic capacity, where only three numerical integrations are required to solve the expression rather than $6 \times N_p \times N_p$ originally.

4. Area spectral efficiency and energy efficiency

ASE is an important parameter for any network engineer. Higher ASE values indicate better utilization of the available bandwidth, which is an expensive and scarce resource. ASE can be expressed, for the unit frequency reuse factor, as [19]:

$$\text{ASE} = \frac{LC}{A} \qquad \left[bits/sec/Hz\right], \tag{19}$$

where L is the total number of users in a cell, C is the ergodic capacity as given in Eq. (11), and A is the area of a cell.

The EE can be estimated as [20]:

$$EE = \frac{P_T + P_C}{WLC} \qquad \left[J/bit\right], \tag{20}$$

where P_T is the transmit power consumed by the base station, which includes the power consumed by the power amplifier and the feeder losses. P_C is the circuit power, which includes the power consumed by hardware such as signal processors, rectifiers, air-conditioning units, and backup batteries. Note that P_T and P_C are independent of each other. W is the bandwidth utilized by the BS.

5. Numerical results and discussion

In this work, we found that the ASE of MC-CDMA systems increases with SNR for both low and high traffic scenarios, as shown in Figure 2. However, the high traffic scenario has a higher ASE as compared to the low traffic scenario for the same SNR. The difference is due to the fact that at low traffic rates the available channel resources are not being fully utilized. The rate of increase of ASE also increases with SNR; this is in contrast to OFDM [18], where the rate of increase decreases with SNR. This is because of intracell interference, which becomes the dominant impairment at high SNR. Since MC-CDMA offers inherent orthogonality, it does not suffer from high intracell interference. At high traffic rates, ASE increases from 0.03 to 0.08 [b/s/Hz] when SNR is increased from 10 to 20 db, i.e. a 2.7 times increase. A similar increase is also observed at low traffic rates, where it increases from 0.005 to 0.015 for the same increase in SNR. This also shows that interference between cells is not a dominant impairment, as otherwise the increasing traffic would not see a similar increase in ASE.

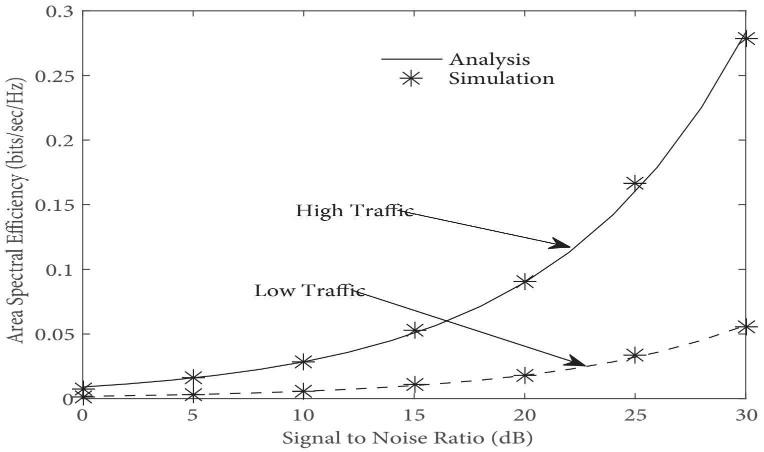

Figure 2. Comparison of low and high traffic ASE with increasing SNR.

Figure 3 shows improvements in EE for both low and high traffic scenarios with increasing SNR. The high traffic scenario performs better than the low traffic scenario with increasing SNR. The EE improves from 180 to 60 [mJ/bit] when SNR increases from 10 to 20 db at a low traffic rate, i.e. 3 times reduction. At high traffic rates, EE improves from 30 to 10 [mJ/bit] for the same increase in SNR, a 3 times reduction. This also confirms that the relative improvement is the same for both low and high traffic scenarios as opposed to OFDM [18], where increasing traffic increases interference.

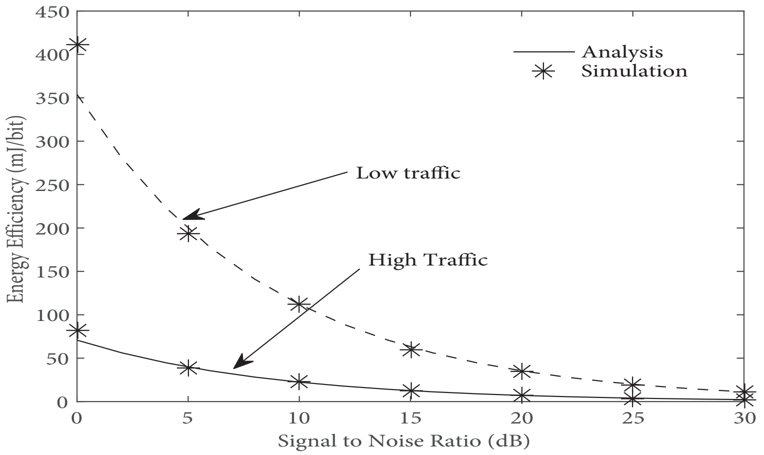

Figure 3. Comparison of low and high traffic EE with increasing SNR.

Figure 4 shows the trade-off between EE and ASE for two values of BS separation (R). The trade-off does not change when the traffic condition changes from low to high, since relative gains are the same, as discussed earlier. However, when the cell size is reduced the ASE increases significantly because the statistical average distance of the user from the BS is reduced. When R is arbitrarily reduced the ASE does not continue to increase due to increased interference, as given in the third term in Eq. (18). Therefore, small cells as envisaged in 5G cellular networks would improve the ASE and EE if MC-CDMA were employed; however, this increase would not be arbitrary.

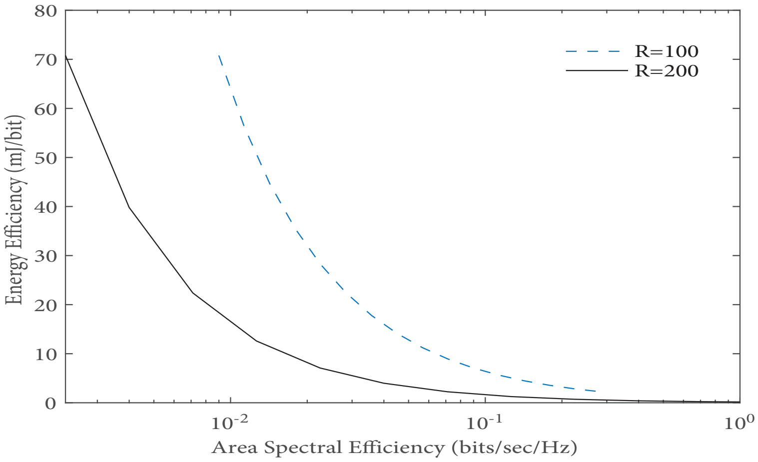

Figure 4. Area spectral efficiency vs. energy efficiency for different intercell distances.

6. Conclusion

ASE and EE are important design parameters in a cellular wireless communication system. We have derived a novel simplified expression for ergodic capacity, requiring only three numerical integrations as compared to $6 \times N_p \times N_p$ otherwise. The new expression leads us to expressions for ASE and EE, and we also confirmed their accuracy using Monte Carlo simulation. Using these expressions we found that both ASE and EE improve at higher traffic load conditions at all SNR values. However, the rate of improvement of both ASE and EE is the same for both traffic scenarios, because of the inherent orthogonality offered by MC-CDMA. Furthermore, smaller cell sizes give higher ASE for the same EE, or conversely better EE for the same ASE. Therefore, MC-CDMA can be a good choice for a design engineer for 5G cellular wireless networks in comparison to OFDM.

References

[1] Jang WM, Nguyen L, Lee MW. MAI and ICI of asynchronous uplink MC-CDMA with frequency offset. IEEE T Veh Technol 2008; 57: 2164-2179.

[2] Wojuola OB, Mneney SH, Srivastava V. Performance of DS-CDMA and MC-CDMA systems in Gaussian and Rayleigh fading channels. In: IEEE International Conference on Computational Intelligence and Computing Research (ICCIC); December 2015. New York, NY, USA: IEEE. pp. 1-6.

[3] Khatri AK, Tharani L. An approach to compare the developments in performance of multicarrier CDMA system. In: International Conference on Computing, Communication Automation; May 2015. pp. 1226-1231.

[4] Luna-Rivera JM, Campos-Delgado DU, Gutierrez CA, Covarrubias-Rosales DH. Performance analysis of closed-loop pre-equalisation for multiuser multiple-input multiple output with multicarrier code division multiple access systems. IET Commun 2016; 10: 235-244.

[5] Rohini S, Suriyakala CD. Effectiveness and performance analysis of MC-CDMA system. In: International Conference on Control, Instrumentation, Communication and Computational Technologies; December 2015. pp. 533-538.

[6] Tomba L, Krzymien WA. Effect of carrier phase noise and frequency offset on the performance of multicarrier CDMA systems. In: IEEE International Conference on Communications; 1996. New York, NY, USA: IEEE. pp. 1513-1517.

[7] Jang WM, Nguyen L, Bidarkar P. MAI and ICI of synchronous downlink MC-CDMA with frequency offset. IEEE T Wirel Commun 2006; 5: 693-703.

[8] Tomba L, Krzymien WA. Sensitivity of the MC-CDMA access scheme to carrier phase noise and frequency offset. IEEE T Veh Technol 1999; 48: 1657-1665.

[9] Gui X, Ng TS. Performance of asynchronous orthogonal multicarrier CDMA system in frequency selective fading channel. IEEE T Commun 1999; 47: 1084-1091.

[10] Jang J, Lee KB. Effects of frequency offset on MC/CDMA system performance. In: IEEE Conference on Vehicular Technology; 1999. New York, NY, USA: IEEE. pp. 566-570.

[11] Taeyoung K, Kyunbyoung K, Youngju K, Daesik H. Performance evaluation of uplink MC-CDMA systems with residual frequency offset. IEICE T Commun 2006; 89: 1455-1458.

[12] Park J, Kim J, Choi S, Cho N, Hong D. Performance of MC-CDMA systems in nonindependent Rayleigh fading. In: IEEE International Conference on Communications; 1999. New York, NY, USA: IEEE. pp. 506-510.

[13] Marsan MA, Chiaraviglio L, Ciullo D, Meo M. Optimal energy savings in cellular access networks. In: IEEE International Conference on Communications Workshops; 2009. New York, NY, USA: IEEE. pp. 1-5.

[14] Auer G, Giannini V, Desset C, Godor I, Skillermark P, Olsson M, Imran MA, Sabella D, Gonzalez MJ, Blume O et al. How much energy is needed to run a wireless network? IEEE Wirel Commun 2011; 18: 40-49.

[15] Mancuso V, Alouf S. Reducing costs and pollution in cellular networks. IEEE Commun Mag 2011; 49: 63-71.

[16] Ashraf I, Boccardi F, Ho L. Power savings in small cell deployments via sleep mode techniques. In: International Symposium on Personal, Indoor and Mobile Radio Communications Workshops; 2010. New York, NY, USA: IEEE. pp. 307-311.

[17] Jiang J, Dianati M, Imran MA, Tafazolli R, Chen Y. On the relation between energy efficiency and spectral efficiency of multiple-antenna systems. IEEE T Veh Technol 2013; 62: 3463-3469.

[18] Aldosari MM, Hamdi KA. Trade-off between energy and area spectral efficiencies of cell zooming and BSs cooperation. In: International Conference on Intelligent and Advanced Systems; 2014. New York, NY, USA: IEEE. pp. 1-6.

[19] Alouini MS, Goldsmith AJ. Area spectral efficiency of cellular mobile radio systems. IEEE T Veh Technol 1999; 48: 1047-1066.

[20] Deng L, Rui Y, Cheng P, Zhang J, Zhang Q, Li M. A unified energy efficiency and spectral efficiency tradeoff metric in wireless networks. IEEE Commun Lett 2013; 17: 55-58.